THE JOURNAL OF BIOLOGICAL CHEMISTRY VOL. 286, NO. 35, pp. 30670–30679, September 2, 2011

Human Fatty Acid Transport Protein 2a/Very Long Chain Acyl-CoA Synthetase 1 (FATP2a/Acsvl1) Has a Preference in Mediating the Channeling of Exogenous n-3 Fatty Acids into Phosphatidylinositol*

Received for publication, January 31, 2011, and in revised form, July 11, 2011 Published, JBC Papers in Press, July 15, 2011, DOI 10.1074/jbc.M111.226316

Elaina M. Melton[‡§], Ronald L. Cerny[¶], Paul A. Watkins[‖], Concetta C. DiRusso[‡], and Paul N. Black[‡1]

From the Departments of [‡]Biochemistry and [¶]Chemistry, University of Nebraska, Lincoln, Nebraska 68588, the [§]Center for Cardiovascular Sciences, Albany Medical College, Albany, New York 12208, and the [‖]Kennedy Krieger Research Institute, Baltimore, Maryland 21205

The trafficking of fatty acids across the membrane and into downstream metabolic pathways requires their activation to CoA thioesters. Members of the fatty acid transport protein/very long chain acyl-CoA synthetase (FATP/Acsvl) family are emerging as key players in the trafficking of exogenous fatty acids into the cell and in intracellular fatty acid homeostasis. We have expressed two naturally occurring splice variants of human FATP2 (Acsvl1) in yeast and 293T-REx cells and addressed their roles in fatty acid transport, activation, and intracellular trafficking. Although both forms (FATP2a (M_r 70,000) and FATP2b (M_r 65,000 and lacking exon3, which encodes part of the ATP binding site)) were functional in fatty acid import, only FATP2a had acyl-CoA synthetase activity, with an apparent preference toward very long chain fatty acids. To further address the roles of FATP2a or FATP2b in fatty acid uptake and activation, LC-MS/MS was used to separate and quantify different acyl-CoA species (C14–C24) and to monitor the trafficking of different classes of exogenous fatty acids into intracellular acyl-CoA pools in 293T-REx cells expressing either isoform. The use of stable isotopically labeled fatty acids demonstrated FATP2a is involved in the uptake and activation of exogenous fatty acids, with a preference toward n-3 fatty acids (C18:3 and C22:6). Using the same cells expressing FATP2a or FATP2b, electrospray ionization/MS was used to follow the trafficking of stable isotopically labeled n-3 fatty acids into phosphatidylcholine and phosphatidylinositol. The expression of FATP2a resulted in the trafficking of C18:3-CoA and C22:6-CoA into both phosphatidylcholine and phosphatidylinositol but with a distinct preference for phosphatidylinositol. Collectively these data demonstrate FATP2a functions in fatty acid transport and activation and provides specificity toward n-3 fatty acids in which the corresponding n-3 acyl-CoAs are preferentially trafficked into acyl-CoA pools destined for phosphatidylinositol incorporation.

Most evidence to date supports the notion that the distribution and trafficking of fatty acids into complex lipids of cells and tissues is non-random and is distinct and characteristic of a specific cell type or an intracellular compartment. How these distinct patterns are generated and maintained is poorly understood, but it is reasonable to expect that the source of the fatty acid, either from endogenous or exogenous sources, will lead to different metabolic fates. These processes are likely governed by proteins and enzymes, which function in fatty acid uptake and metabolic trafficking. Previously it has been very difficult to distinguish these fatty acid trafficking events, but advances in mass spectrometry has provided the requisite tools to resolve these outstanding questions and to define the role(s) of specific proteins involved in metabolic trafficking. In this work we have employed stable isotopically labeled fatty acids to address the roles of the human fatty acid transport proteins in fatty acid uptake, activation, and trafficking into complex lipids.

Different members of the fatty acid transport protein/very long chain acyl-CoA synthetase (FATP/Acsvl)[2] and long chain acyl-CoA synthetase (Acsl) families of proteins are emerging as likely players in both fatty acid transport and intracellular trafficking (1–4). All Acsl isoforms and many FATP isoforms activate fatty acid to yield acyl-CoA; in the context of fatty acid transport, one mechanism that is operational is vectorial acylation, which results in the formation of acyl-CoA concomitant with transport (1). In *Escherichia coli*, a single Acsl functions in this process by activating in excess of 98% of exogenous fatty acid to acyl-CoA, thereby linking transport with downstream metabolism. This enzyme also functions in intracellular fatty acid trafficking and phospholipid turnover as part of normal fatty acid homeostasis (5–7). Evidence for vectorial acylation as a mechanism driving fatty acid import in eukaryotic cells is less well defined. In the context of fatty acid activation, the Acsls have highest activity toward C16-C20 fatty acids and display some discrimination with regard to saturation (2, 4, 8). The FATPs, by comparison, activate very long and branched chain fatty acids, and several also function in the transport of long chain fatty acids and thus have distinguishing transport and activation substrate preferences for each process (1, 4, 9–25). In both yeast and adipocytes, there is evidence that specific FATP and Acsl isoforms form a complex that functions in vectorial

* This work was supported, in whole or in part, by National Institutes of Health Grants RO1-DK07076 and RO1-GM56850 (to P. N. B. and C. C. D.) and 1F31DK085961 (to E. M. M.).

[1] To whom correspondence should be addressed: Dept. of Biochemistry, N200 George W. Beadle Center, University of Nebraska, Lincoln, NE 68588-0664. Tel.: 402-472-3212; E-mail: pblack2@unl.edu.

[2] The abbreviations used are: FATP, fatty acid transport protein; Acsvl, very long chain acyl-CoA synthetase; ESI, electrospray ionization; PC, phosphatidylcholine; PI, phosphatidylinositol.

acylation to allow long chain fatty acid uptake and activation to occur coordinately (19, 25).

Recent studies in mammalian systems suggest the FATP and Acsl isoforms provide central roles in metabolic movement of fatty acids into complex lipid pools (26). Overexpression studies examining the function of Acsl1, for example, demonstrated that this enzyme provides an important role in triglyceride synthesis in cardiac myocytes, hepatocytes, and NIH 3T3 cells (27–29). Triacsin C (an Acsl inhibitor) treatment results in a marked decrease in long acyl-CoA synthetase activity in fibroblasts that parallels with a decrease in fatty acid incorporation into triglyceride (30). Knockdown studies of Acsl5 in hepatocytes results in reduced exogenous fatty acid incorporation into triglycerides, phospholipids, and cholesterol esters (31). Members of the FATP family have significant homologies to the Acsls and indeed function in the activation of very long chain fatty acids (10). The overexpression of FATP1 in 293 cells channels exogenous fatty acids into triglyceride synthesis (32). Taken together, it is clear the different FATP and Acsl isoforms have unique functions in fatty acid partitioning and downstream metabolism and thus provide different roles in maintaining fatty acid homeostasis (33).

To investigate the roles of human FATP2 and a unique splice variant, FATP2b, in fatty acid uptake and downstream metabolism, we have employed fatty acids labeled with stable isotopes and traced their metabolic fates using high resolution mass spectrometry. Previous studies on the FATPs and Acsls have been hampered by the inability to monitor and distinguish unique metabolic pools of endogenous *versus* exogenous fatty acids. However, the development of highly sensitive mass spectrometry techniques to monitor the metabolism of substrates labeled with stable isotopes affords the opportunity to investigate the dynamic nature of the metabolome (34–36). For example these approaches have been used to identify and quantify specific biomarkers for various disease states (35, 37–39). In this work, different classes of fatty acids labeled with C13 or deuterium have been used to monitor the formation of acyl-CoA and downstream metabolic trafficking in cells expressing FATP2a or FATP2b. These studies revealed novel insights into the roles provided by these members of the FATP family of proteins in determining the selectivity and specificity of acyl-CoA formation from exogenous fatty acids and their subsequent trafficking into complex lipids. Of particular note was the finding that FATP2a has a unique metabolic phenotype with a preference for generating CoA derivatives of n-3 fatty acids, which are preferentially trafficked into phosphatidylinositol.

EXPERIMENTAL PROCEDURES

Generation of Yeast Cells Expressing FATP2a and FATP2b—Watkins *et al.* (40) first described FATP2a as very long chain acyl-CoA synthetase Acsvl1 (FATP2 variant 1, NCBI reference sequence NM_003645.3). FATP2b, obtained from the Image Consortium library (clone 30348317; FATP2 variant 2, NCBI reference sequence NM_001159629.1) lacks exon 3, which encodes a region of the protein that contains part of the ATP binding domain and is required for adenylate formation (ATP/AMP motif). *Saccharomyces cerevisiae* strain LS2086 containing deletions within the *FAT1* and *FAA1* genes (*fat1*Δ*faa1*Δ; *MATa ura3 52 his3200 ade2-101 lys2-801 leu2-3,112 faa1*Δ::*HIS3 fat1*Δ::*G418*) were transformed with pDB121-derived plasmids expressing FATP2a (pDB128) or FATP2b (pDB126) along with the GAL4 transcription factor fusion vector, pRS416Gal4-ER-VP16. Transformation of yeast used standard lithium acetate procedures (41). The details of pDB126 have been previously described (24). pDB128 was generated by PCR amplification of the cDNA containing human Acsvl1 (40) using primers 5′-GC ATA GCC CTC GAG ATG CTT TCC GCC ATC TAC ACA-3′ and 5′-CGC AGA CCA AGC TTT CAG AGT TTC AGG GTT TTA GC-3′, which resulted in XhoI and HinDIII restriction sites, respectively. Cloning FATP2a and FATP2b into pDB121 facilitated expression from the galactosidase promoter of a T7-tagged fusion protein, which allows detection. Plasmids were propagated in *E. coli* strain DH5α and the sequences of both clones were verified. Yeast cells were grown in yeast minimal medium with dextrose containing 0.67% yeast nitrogen base, 2% dextrose, adenine (20 mg/liter), and uracil (20 mg/liter), and the following amino acids were added as required: 20 mg/liter arginine, tryptophan, methionine, histidine, and tyrosine, 30 mg/liter lysine, and 100 mg/liter leucine). For expression of FATP2a and FATP2b, the cells were subcultured to a A_{600} of 0.02 in the same medium containing 10 nM β-estradiol, grown to mid-log-phase (0.8–1.2 A_{600}), harvested, and then resuspended in PBS to a final density of 6×10^7 cells/ml before dispensing into a 96-well assay plate for transport measurements or collected by centrifugation for Western blots or acyl-CoA synthetase measurements.

Generation of 293T-REx Stable Cell Lines Allowing the Controlled Expression of FATP2a and FATP2b—The coding sequences for FATP2a and FATP2b were amplified by PCR using the primers 5′-GCA TAG CCA AGC TTG ATG CTT TCC GCC ATC TAC AC-3′ and 5′-CGC AGA CCC TCG AGG AGT TTC AGG GTT TTA GCA CT-3′ generating HinDIII and XhoI restriction sites, respectively, from the yeast expression clones (detailed above), cloned into pcDNA4/TO/myc-His (Invitrogen), and propagated in *E. coli* strain JM109; the sequences of both expression clones were verified. Stable 293T-REx cell lines (Invitrogen; stably expressing the tetracycline repressor protein) expressing FATP2a and FATP2b were generated as follows. Cells were seeded at 1×10^6 cells in 60-mm dishes in DMEM medium containing 10% FBS and 5 μg/ml blasticidin; 24 h after seeding cells were transfected with 30 μg of pcDNA4 FATP2a (pDB312), pcDNA4 FATP2b (pDB311), LacZ (control), or empty vector (control) using 293 Fectin (Invitrogen). 24 h post-transfection 125 μg/ml zeocin was added to the media. 48 h after transfection the cells were reseeded at 5.0×10^3 cells/cm^2 in 6-well plates containing fresh medium supplemented with 5 μg/ml blasticidin and 125 μg/ml zeocin. The selective medium was replaced every 3–4 days until foci were visible. Several clones of each were isolated using cloning rings and expanded into 96-well plates. When cells were more than 90% confluent they were split 1:3 in the same surface area; the cells were subsequently expanded into a larger surface area using a 12-well plate.

Induction of expression of FATP2a or FATP2b was accomplished by the addition of tetracycline to a final concentration

of 2 μg/ml for 48 h; the cells were harvested and then subjected to analytical studies as detailed below. Proteins expressed from the pcDNA4 vector contain a c-*myc* epitope tag, which facilitated expression monitoring using Western blots, and a c-*myc* antibody.

Fatty Acid Transport—The patterns of fatty acid transport were monitored using the live cell, real-time method by measuring the accumulation of the fluorescently labeled long chain fatty acid, 4,4-difluoro-5-methyl-4-bora-3a,4a-diaza-*s*-indacene-3-dodecanoic acid, C_1-BODIPY-C_{12}, employing trypan blue as the extracellular quenching agent (42).

To monitor fatty acid transport in yeast, strain LS2086 was co-transformed with the pDB121-derived constructs expressing FATP2a or FATP2b and pRS416Gal4-ER-VP16. Cells were grown as detailed above and resuspended in PBS to a final density of 6×10^7 cells/ml before dispensing into a 96-well assay plate (75 μl/well). 75 μl of the C_1-BODIPY-C_{12} transport mixture (2.5 μM C_1-BODIPY-C_{12}, 1.5 μM fatty acid-free BSA, 4 mM Trypan blue) were added to each well. The cell-associated fluorescence, reflective of fatty acid transport, was measured using a Bio-Tek Synergy HT multidetection microplate reader (Bio-Tek Instruments, Inc. Winooski, VT) using filter sets of 485 ± 20 nm excitation and 528 ± 20 nm emission. Data are expressed as arbitrary fluorescence units/3×10^6 cells/30 min.

The roles of FATP2a and FATP2b in fatty acid transport were defined using the stable 293T-REx cell lines grown under standard conditions in the presence of tetracycline (2 μg/ml) (see above) in optically transparent 96-well plates. Cells were seeded at 50,000 cells per 96-well in standard media containing 5 μg/ml blasticidin and 125 μg/ml zeocin. 24 h after plating 2 μg/ml tetracycline was added to the cells for induction. 48 h post-induction cells were serum-starved for 1 h in minimum Eagle's medium without phenol red (50 μl) before performing the C_1-BODIPY-C_{12} transport assay (42). Subsequently, 50 μl of the C_1-BODIPY-C_{12} mixture (varying concentrations of C_1-BODIPY-C_{12} (0.5–32 μM as detailed in Fig. 3*A*), 10 μM fatty acid-free BSA, 4 mM trypan blue) was added to each well, and transport was determined by measuring the cell-associated fluorescence as detailed above. Data were expressed as arbitrary fluorescence units/min/10^6 cells. The cell number in each well was determined using a standard Hoechst assay used to quantify DNA. The fluorescence was read at 350/450 nm (excitation/emission). The cell number was calculated from a standard curve generated for cell number *versus* fluorescence units.

Acyl-CoA Synthetase Activity Determinations—Yeast cells and 293T-REx cells expressing FATP2a or FATP2b were grown under inducing conditions as detailed above. For acyl-CoA synthetase determination, yeast cells were collected by centrifugation (5000 × *g*, 15 min); the media in the 293T-REx cells was aspirated off, and cells washed once with 5 ml of PBS, trypsinized using standard procedures, and collected by centrifugation. The cell pellets (yeast or 293T-REx cells) were resuspended in 1 ml of STE lysis buffer (10 mM Tris-HCl, pH 8.0, 100 mM NaCl, 1 mM EDTA) and sonicated to lyse the cells on ice. Samples were clarified by centrifugation (5000 × *g*, 15 min); supernatants were transferred to new tubes and assayed for acyl-CoA synthetase activities as detailed below; protein concentrations were determined using the Bradford assay using bovine serum albumin as a standard.

Acyl-CoA synthetase activities were determined using a reaction mixture containing 50 mM Tris-HCl, pH 8.0, 10 mM ATP, 10 mM $MgCl_2$, 0.01% Triton X-100, 0.3 mM DTT, 50 μM [^{3}H]oleic acid ($C_{18:1}$) or [^{3}H]lignoceric acid ($C_{24:0}$) (dissolved in 10 mg/ml α-cyclodextrin). The addition of coenzyme A (to a final concentration of 0.2 mM) initiated the reaction. Samples were incubated at 30 °C for 20 min, and the reaction was terminated by the addition of 2.5 ml of Dole's reagent (isopropyl alcohol, *n*-heptane, 1 M H_2SO_4 (40:10:1)) (43). The unesterified fatty acid was removed through organic extraction using *n*-heptane. Acyl-CoA formed during the reaction remained in the aqueous fraction and was quantified by scintillation counting. Data were expressed as nmol or pmol of acyl-CoA formed/min/mg of protein.

Western Blotting to Monitor Protein Expression—The expression of FATP2a and FATP2b was monitored using Western blot analysis using α*c-myc* (Invitrogen) or αT7 (Invitrogen) coupled with the appropriate secondary antibodies. The concentrations of the primary and secondary antibodies were used as recommended by the manufacturer or experimentally determined. Detection was accomplished using enhanced chemiluminescence.

Expression Patterns of FATP2a and FATP2b Assessed Using RT-PCR—RT-PCR was used to detect the expression of FATP2a and FATP2b in eight different human tissues. cDNAs used in the PCR reactions were prepared from total RNA from brain, liver, placenta, and heart (obtained from BioChain, Hayward, CA). Total RNA (1 μg) was used to synthesize cDNA using the Bio-Rad I-script cDNA synthesis kit according to manufacturer's conditions. The parameters for cDNA synthesis were 25 °C (5 min), 42 °C (30 min), and 85 °C (5 min). Fully synthesized cDNAs were from colon, white adipose tissue, small intestine, and kidney were also obtained from BioChain. PCR was performed using the oligonucleotide pairs 5′-CAA CTG AAC CTA TCC CAG AG-3′ (forward primer) and 5′-CTG AAT GAC AGT GAC GTT G-3′ (reverse primer). These primers were designed to amplify regions upstream and downstream of exon 3, which provided a distinction between the FATP2a and FATP2b PCR products. PCR products were expected to be 326 bp (FATP2a, exon 3 present) and 167 bp (FATP2b, exon 3 is missing). PCR was performed using 1 μl of the cDNA mixture (prepared as detailed above or obtained commercially), 0.5 μM concentrations of each oligonucleotide primer, 0.2 mM dNTPs, and 1 unit of Taq polymerase (Roche Applied Science) in a final volume of 50 μl. PCR parameters included: 95 °C (5 min) followed by 35 cycles of 30 s (95 °C), 30 s (46 °C), and 45 s (72 °C); the final extension step was held at 72 °C for 10 min. The PCR products were resolved using non-denaturing polyacrylamide gel electrophoresis and visualized using ethidium bromide.

Stable Isotope Labeling and Fatty Acyl-CoA Extraction—For stable isotope labeling experiments, 293T-REx cells were cultured and induced as described above. 48 h after induction with tetracycline, the cells were starved for 1 h in serum-depleted minimum Eagle's medium. The cells were then treated with 50 μM U-^{13}C- or ^{2}H-labeled fatty acids for 4 h ([U-^{13}C]C16:0

(Cambridge Isotope Laboratories, Inc.), [U-^{13}C]C18:0 (Isotec/Sigma), [U-^{13}C]C18:1 (Medical Isotope, Inc.), [U-^{13}C]C18:2 (n-6) (Cambridge Isotope Laboratories, Inc.), [U-^{13}C]C18:3 (n-3) (Medical Isotope, Inc.), [$^{2}H_{8}$]C20:4 (n-6) (Isotec/Sigma), [$^{2}H_{5}$]C22:6 (n-3) (Isotec/Sigma), and [$^{2}H_{47}$]C24:0) (C/D/N isotopes, Inc.). After treatment with stable isotopically labeled fatty acids, the cells were then washed with 100 μM BSA in Hanks' buffer. To collect the sample for fatty acyl-CoA analysis, cells were scraped off the culture dish, resuspended in 5 ml of PBS, and then harvested by centrifugation. The cell pellets were resuspended in 0.5 ml of water, and 0.2 ml of the cell suspension was immediately put on ice for fatty acyl-CoA extraction. Fatty acyl-CoA extraction methods were adopted from Haynes *et al.* (36). In brief, the cells were sonicated for 30 s after the addition of 0.5 ml of 1 mM EDTA in methanol. Chloroform (0.25 ml) and 100 pmol of each internal standard (C17:0 CoA, C19:0 CoA, and C23:0 CoA) were added to each sample. The cells were sonicated again for 30 s and then incubated in a 50 °C water bath for 30 min. After the addition of chloroform (0.25 ml) and water (0.25 ml), the mixture was vortexed and centrifuged at 3000 rpm for 5 min. The upper phase was collected, and 0.5 ml of water/methanol/chloroform (45:50:5 (v/v)) was added to the bottom phase followed by centrifugation for phase separation. This step was repeated one additional time to extract additional acyl-CoAs from the samples. Finally, 0.18 ml methanol/butanol/chloroform (50:25:25) mixture was added, and the fatty acyl-CoA extracts were stored at −80 °C until analyzed by LC-electrospray ionization tandem mass spectrometry (LC-ESI/MS/MS).

LC-ESI/MS/MS Analysis of Fatty Acyl-CoA—Fatty acyl-CoAs were separated by reverse phase HPLC using a C18 reverse phase column (Phenomenex Gemini; 2 × 150 mm, 5-μm particle size) applying a binary flow of 0.25 ml/min at 40 °C. Elution gradient steps were as follows: 100% A, 5 min; gradient to 60% B, 5 min; gradient to 100% B, 1 min; 100% B, 5 min on a Shimadzu system as previously detailed (36). Buffer A (water/acetonitrile (85:15) 0.05% triethylamine (TEA)) and Buffer B (water/acetonitrile (10:90), 0.05% TEA) were used as the mobile phases. A Phenomenex Gemini guard column (2 × 4 mm) was routinely used to prefilter the acyl-CoA extracts. The injection volume for LC-ESI/MS/MS analysis was 30 μl. The C18 column was re-equilibrated with 100% A for 5 min between runs.

Fatty acyl-CoAs were detected and quantified using (ESI/MS/MS) in the positive ion mode using a linear ion trap quadrupole mass spectrometer (4000 QTrap; AB Sciex Instruments) that was operated using the methods previously described (36, 44) with some modifications. Under these conditions, the fatty acyl-CoAs fragments into fatty acylpantethine and phosphoadenosine diphosphate. To monitor the different acyl-CoA species, the MS scans for ions that have a neutral loss of 507 Da, which corresponds to the loss of the phosphoadenosine diphosphate group. Multiple reaction monitoring scans were set up to detect the precursor ion $(M+H)^+$ and the product ion that results after fragmentation of each particular acyl-CoA. The ion pairs monitored for fatty acyl-CoA standards and stable isotopically labeled CoAs are detailed in Table 1. For total acyl-CoA profile analysis, each CoA species was quantified using standard curve measurements produced for each individual acyl-CoA. To quantify labeled CoAs enrichments, peak areas for these unique analytes were compared with peak areas of the internal standard CoAs (C17:0-CoA, C19:0-CoA, and C23:0-CoA). Analyte monitoring and quantification were conducted with Analyst 1.5 Software from AB Sciex.

TABLE 1

Multiple reaction monitoring pairs and ESI/MS conditions for fatty acyl-CoA species monitored by ESI/MS/MS

Multiple reaction monitoring scans were in the positive ion mode; dwell time for each analyte was 80 ms. DP, declustering potential; CE, collision energy; CXP, collision cell exit potential; RT, retention time (min); $n = 3$.

Fatty acyl-CoA	Q1 mass	Q3 mass	DP, CE, CXP	LC RT (±S.E.)
	Da	*Da*	*eV*	*min*
Internal standards				
C17:0-CoA	1020.4	513.4	200, 54, 14	13.08 (0.27)
C19:0-CoA	1048.4	541.4	200, 54, 14	13.71 (0.20)
C23:0-CoA	1104.5	597.5	200, 54, 15	14.84 (0.27)
Stable isotopically labeled fatty acyl-CoA				
[U-^{13}C]C16:0-CoA	1022.4	515.4	200, 54, 11	12.84 (0.27)
[U-^{13}C]C18:0-CoA	1052.4	545.4	200, 53, 14	13.21 (0.12)
[U-^{13}C]C18:1-CoA	1050.4	543.3	200, 54, 14	13.29 (0.10)
[U-^{13}C]C18:2-CoA	1048.4	541.4	200, 54, 14	12.52 (0.09)
[U-^{13}C]C18:3-CoA	1046.4	539.4	200, 54, 11	13.13 (0.21)
[$^{2}H_{8}$]C20:4-CoA	1062.4	555.4	210, 55, 15	13.01 (0.16)
[$^{2}H_{5}$]C22:6-CoA	1083.4	576.4	200, 54, 14	12.25 (0.15)
[$^{2}H_{47}$]C24:0-CoA	1165.4	658.5	210, 54, 14	15.07 (0.26)

ESI/MS Analysis of Stable Isotopically Labeled Phospholipids—Total lipids were extracted from cells labeled with stable isotopically labeled fatty acids using methods established by Bligh and Dyer (45). A mixture of phospholipid Internal standards (PC 13/13 and PI 16/16) was added to each sample during the first lipid extraction step for subsequent analyte quantification. Total lipid extractions were diluted in solvent A (methanol/isopropyl alcohol/water (70:5:25), 10 mM ammonium formate) to a final dilution of 1:50. Phospholipids were analyzed with a linear ion trap quadrupole mass spectrometer (4000 QTrap) manufactured by AB Sciex Instruments. This system is also equipped with two Shimadzu LC20ADXR LC pumps, a Shimadzu CBM20A LC controller, and a Shimadzu SIL20AC autosampler, which allowed samples to be automatically infused into the ESI source using flow injection ESI/MS methods (46–48). Infusion conditions included directly infusing samples into the source using a 50 μl injection loop at a flow rate of 0.05 ml/min with Solvent A and Solvent B (methanol/isopropyl alcohol/water (94:5:1), 10 mM ammonium formate) as the mobile phases. To monitor PC species, precursor scans were conducted in the positive ion mode to detect precursor ions of m/z 184. The 184 ion corresponds to the head group of PC, which results after fragmentation. PI molecular species were analyzed by neutral loss scanning for ions that result from the neutral loss of 277 m/z, which corresponds to the loss of the PI head group. Fatty acid composition was determined for PC and PI molecular species that exhibited a mass that corresponded to a species that was labeled with a stable isotope labeled fatty acid. PC and PI species labeled with [$^{2}H_{5}$]C22:6 had a mass of M+5, whereas those labeled with [U-^{13}C]C18:3 had a mass of M+18. Fatty acid fragments from these unique peaks were analyzed by MS/MS scans to confirm fatty acid incorporation into PC and PI species. Analyte monitoring and quantification are conducted with Analyst Version 1.5 Software

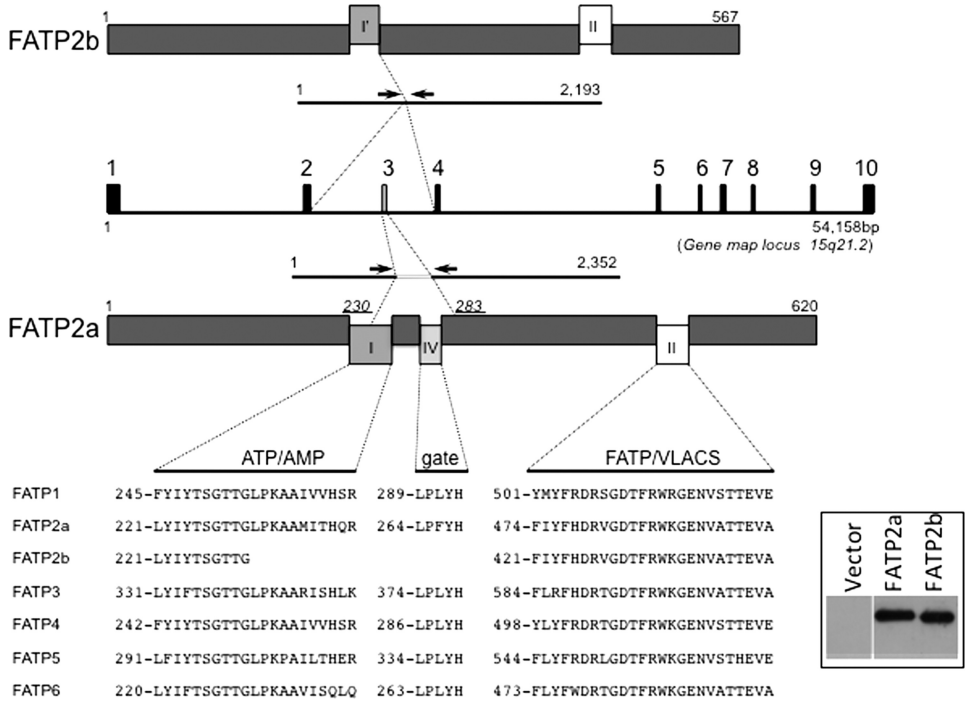

FIGURE 1. **Organization of FATP2a and FATP2b.** Shown is an overview of FATP2a and FATP2b in relationship to the FATP2 gene. *I* represents the ATP/AMP motif; *IV* is the gate region; *II* is the FATP/VLACS motif (*upper*); shown is alignment of amino acid sequences of human FATPs in regions (I (ATP/AMP motif), II (FATP/VLACS motif), and IV (gate)). The *numbers* refer to the first amino acid residue in the selected regions. *Inset*, expression of FATP2a and FATP2b in yeast using Western blots of the *fat1*Δ *faa1*Δ strain of yeast expressing FATP2a and FATP2b probed with anti-T7 in relationship to the vector control.

from AB Sciex and the Online LipidomeDB Data Calculation Environment, developed and managed by the Kansas Lipidomics Research Center and K-INBRE Bioinformatics Core Facility to quantify phospholipid molecular species (49).

RESULTS

Features of FATP2a and FATP2b—Fig. 1 illustrates the genome organization of the human FATP2 (Acsvl1) locus (15q21.2). The gene is 54,158 nucleotides in length and is predicted to contain 10 exons. In comparing the sequences from FATP2a (obtained from liver) and FATP2b (obtained from placenta), we found that the latter lacked exon 3, which encodes part of the core ATP/AMP motif (I) and the gate region (IV). On the basis of directed mutagenesis in a number of different acyl-CoA synthetases and FATPs and the crystal structure of the *Thermus thermophilus* acyl-CoA synthetase, the ATP/AMP motif contributes to ATP binding, whereas the gate provides fatty acid access after nucleotide binding (50–53). The core FATP/Acsvl motif (II), shown to be involved in fatty acid transport in the yeast orthologue, remained intact (51). These data predicted that FATP2b would be unable to activate fatty acids to CoA thioesters.

*Functional Studies of FATP2a and FATP2b When Expressed in the fat1*Δ *faa1*Δ *Strain of Yeast*—To address the roles of FATP2a and FATP2b in both fatty acid transport and fatty acid activation, we generated clones that allowed expression in yeast. As a host, we employed the *fat1*Δ *faa1*Δ yeast strain 1) as it is unable to transport long chain fatty acids, 2) has ~10% wild-type long chain acyl-CoA synthetase activity (contributed by Faa4p)(13), and 3) is unable to activate very long chain fatty acids (11). This provided a well defined heterologous system to distinguish transport and activation functions. Both FATP2a and FATP2b were expressed from the galactosidase promoter as detailed under "Experimental Procedures" as protein fusions with a T7 epitope (Fig. 1, *inset*). As expected, FATP2b was slightly smaller than FATP2a, giving a M_r on SDS gels of 65,000 compared with 70,000 for FATP2a. This was consistent with FATP2b lacking the 53-amino acid segment encoded within exon3. Long chain fatty acid transport was assessed using C_1-BODIPY-C_{12} as a surrogate fatty acid under conditions well established in our laboratory (42). Both FATP2a and FATP2b were proficient in long chain fatty acid transport (Table 2). These data indicated that although FATP2b lacked part of the ATP/AMP motif and the gate region, it could still function in fatty acid transport.

TABLE 2

C_1-BODIPY-C_{12} transport in the yeast *fat1*Δ *faa1*Δ strain expressing human FATP2a or FATP2b

Vector controls are the same cells transformed with pDB121. AFU, arbitrary fluorescence units/3 × 10^6 cells/30 min; $n = 6$.

	AFU (±S.E.)
Vector	680.8 (29.6)
FATP2a	2369.3 (89.2)[a]
FATP2b	2668.7 (41.9)[a]

[a] $p \leq 0.05$ using a paired t test relative to vector control.

We next addressed the contributions of FATP2a and FATP2b to long and very long acyl-CoA synthetase activities. Expression of FATP2a and FATP2b did not increase oleoyl-CoA synthetase activities above the vector control consistent with the conclusion that neither provided long chain acyl-CoA synthetase activity (Table 3). In contrast, only FATP2a was able to activate very long chain fatty acids. These data collectively indicated that FATP2b was catalytically inactive as an acyl-CoA

synthetase, but when expressed in yeast and like FATP2a enhanced the transport of exogenous long chain fatty acids. On the basis of our previous work showing that the yeast FATP (Fat1p) and a long chain acyl-CoA synthetase (Acsl; Faa1p or Faa4p) form a functional complex at the membrane, we suspect that both FATP2a and FATP2b were able to partner with the yeast Acsl Faa4p to promote the transport of long chain fatty acids via vectorial acylation (25). This work verified predictions made using alanine-scanning mutagenesis of yeast Fat1p, which identified specific amino acid residues that distinguished fatty acid transport from very long chain fatty acid activation (51). In the present case we have demonstrated the naturally occurring isoforms FATP2a and FATP2b both function in fatty acid uptake but differ in their ability to activate very long chain fatty acids.

TABLE 3

Acyl-CoA synthetase activities using long chain and very long chain substrates in the yeast *fat1*Δ *faa1*Δ strain expressing human FATP2a or FATP2b

Vector controls are the same cells transformed with pDB121. Data are S.E.; $n = 3$.

	Acyl-CoA synthetase activity (±S.E.)	
	$C_{18:1}$	$C_{24:0}$
	nmol/min/mg protein	*pmol/min/mg protein*
Vector	3.4 (0.3)	1.6 (0.3)
FATP2a	4.4 (0.9)	22.9 (3.2)[a]
FATP2b	4.7 (0.7)	1.2 (0.2)

[a] $p \leq 0.001$ using a paired *t* test relative to vector control.

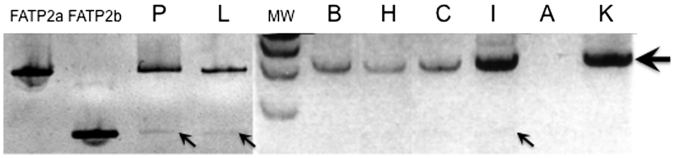

FIGURE 2. **Tissue-specific expression of the FATP2 variants.** RT-PCR using primers illustrated as *arrows* in Fig. 1 of cDNA were prepared from total RNA obtained from placenta (*P*), liver (*L*), brain (*B*), and heart (*H*) and cDNA from colon (*C*), small intestine (*I*), white adipose tissue (*A*), and kidney (*K*); *lanes FATP2b* and *FATP2a* are the controls respectively; *MW* represents the molecular weight markers. The *large arrow* indicates the RT-PCR products corresponding to FATP2a; the *small arrows* highlight the RT-PCR products corresponding to FATP2b.

Tissue Expression Patterns of FATP2a and FATP2b—The original clones for FATP2a and FATP2b were obtained from human liver and placenta, respectively. Using primers flanking exon 3, we used RT-PCR to address whether both splice variants were expressed in eight different tissues, including liver and placenta (Fig. 2). Both forms of FATP2 were expressed in placenta, liver, and intestine; however, the expression of FATP2b was always much lower relative to FATP2a. Although there was expression of FATP2a in brain, heart, colon, and kidney, we were unable to detect reproducible expression of FATP2b. Interestingly there was no expression of either FATP2a or FATP2b in white adipose tissue.

Functional Studies of FATP2a and FATP2b in 293T-REx Cells—To further address the differential activities of FATP2a and FATP2b, we expressed these proteins in 293T-REx cell lines as detailed under "Experimental Procedures." The target gene was cloned into pcDNA4/TO/myc-His, which allowed regulated expression from the Tet promoter. On the basis of array data for the 293T-REx parent line, HEK 293, the expression of FATP2 is very low (54), and thus this cell line was ideal to address the function of these FATP2 variants in a mammalian host. We first assessed the patterns of long chain fatty acid transport using a live cell assay employing the fluorescent long chain fatty acid C_1-BODIPY-C_{12} (Fig. 3*A*). Expression of both FATP2a and FATP2b increased the levels of fatty acid transport, although FATP2a was more proficient (~30% higher when compared with cells expressing FATP2b). The expression of both FATP2a and FATP2b using tetracycline were comparable and were routinely monitored using Western blots (*inset*, Fig. 3*A*).

We next assessed long chain and very long chain acyl-CoA synthetase activities in cells expressing FATP2a or FATP2b (Fig. 3, *B* and *C*). Neither FATP2a nor FATP2b increased long chain acyl-CoA synthetase activity using oleate as a substrate,

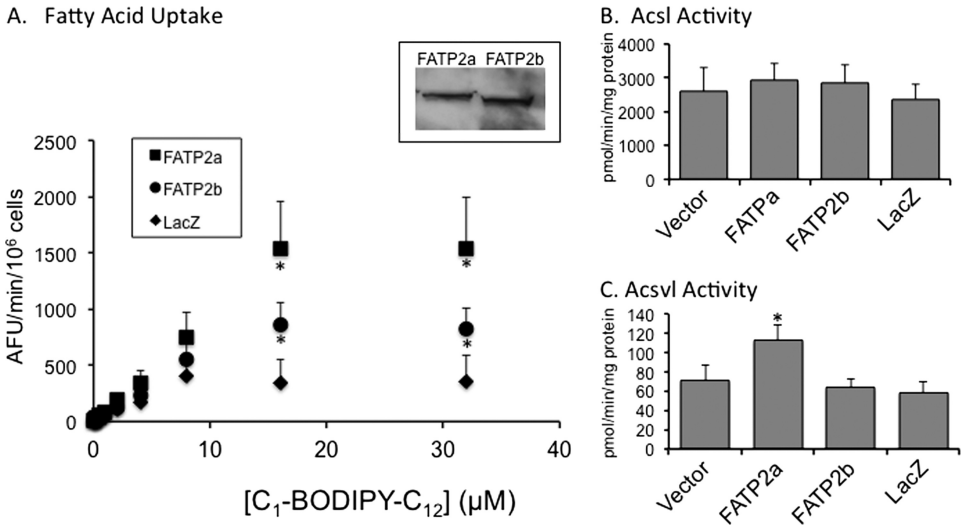

FIGURE 3. *A*, fatty acid transport in 293T-REx cells expressing FATP2a, FATP2b, or LacZ using varying C_1-BODIPY-C_{12} concentrations. The *inset* is a Western blot illustrating expression of FATP2a and FATP2b in 293T-REx cells (using c-*myc* antibody). The *error bars* represent the S.E. ($n = 3$ or 4). *AFU*, arbitrary fluorescence units. Long chain (oleoyl-) (*B*) and very long chain (lignoceryl-) (*C*) CoA synthetase activities in 293T-REx cells expressing FATP2a or FATP2b are shown; the vector and LacZ controls are shown for reference to define background levels. The *error bars* represent the S.E. ($n = 4$). *, $p \leq 0.05$ relative to vector control (paired *t* test).

TABLE 4

Acyl-CoA levels in 293T-REx cells expressing FATP2a or FATP2b

Total acyl-CoA levels were defined for each cell type by summing the levels defined for individual acyl-CoA species shown in Fig. 4.

	Acyl-CoA levels (±S.E.)[a]
	pmol/10⁶ cells
Vector	52.44 (5.95)
FATP2a	63.22 (19.40)
FATP2b	50.58 (13.36)

[a] $n = 3$.

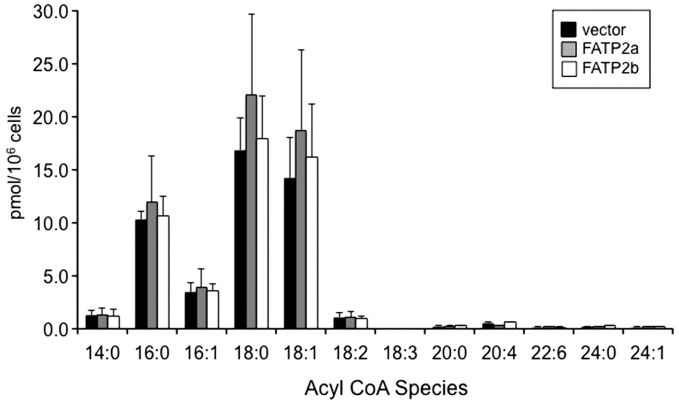

FIGURE 4. **Acyl-CoA profiles of 293T-REx cells expressing FATP2a or FATP2b.** After induction of expression of FATP2a (*gray bars*) or FATP2b (*white bars*), cells were harvested, and acyl-CoAs were extracted as described under "Experimental Procedures." Acyl-CoA extractions were separated and analyzed using LC-ESI/MS/MS (the *black bars* represent cells transformed with vector and also subjected to the same inducing conditions). Individual acyl-CoA levels were calculated from standard curves using AB Sciex Analyst software Version 1.5. The *error bars* represent the S.E. ($n = 5$).

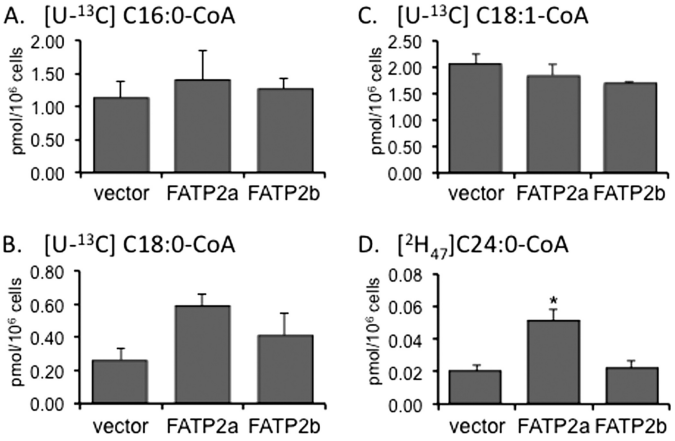

FIGURE 5. **Isotopically labeled acyl-CoA profiles in 293T-REx cells expressing FATP2a or FATP2b.** 293T-REx cells expressing FATP2a or FATP2b were labeled with 50 μM [U-^{13}C]C16:0 (*A*), [U-^{13}C]C18:0 (*B*), [U-^{13}C]C18:1 (*C*), or [$^{2}H_{47}$]C24:0 (*D*) for 4 h, and isotopically labeled acyl-CoAs were determined using LC-ESI/MS/MS as detailed under "Experimental Procedures." The *error bars* represent the S.E. ($n = 3$ or 4). *, $p \leq 0.05$ relative to vector control (paired *t* test).

indicating both lacked this activity. On the other hand, only FATP2a was able to activate very long chain fatty acids, which necessarily requires the ATP binding region of the protein contributed by exon 3 verifying data obtained using the yeast model. Importantly, the finding that FATP2b was catalytically inactive toward very long chain fatty acids but still functioned in the transport of long chain fatty acids is consistent with a probable interaction with a specific Acsl. The yeast FATP mutant S258A-Fat1p lacks very long chain acyl-CoA synthetase activity yet retains the ability to transport the long chain fatty acid oleate (51). In essence, our previous work identified a point mutant in the ATP/AMP motif in the yeast FATP that retains transport activity but is essentially devoid of acyl-CoA synthetase activity; as a naturally occurring variant, FATP2b has many similar characteristics.

Steady State acyl-CoA Levels in 293T-REx Cells Expressing FATP2a or FATP2b—Apart from uptake of exogenous fatty acids, we chose to further assess the roles of FATP2a and FATP2b in endogenous fatty acid metabolism by measuring the steady state levels of the different acyl-CoA species in 293T-REx cells expressing these isoforms using LC-ESI/MS/MS (Table 4; Fig. 4). Considering that the specificity of acyl-CoA synthetase activity attributed to FATP2 is for very long chain fatty acids, we expected the corresponding acyl-CoA species to be increased by overexpression of FATP2a alone. Although the total acyl-CoA levels were increased by ~20% in cells expressing FATP2a when compared with those defined for cells expressing FATP2b or transformed with the vector (Table 4), we could not detect a significantly different amount of any individual species (Fig. 4). This may be because the activated fatty acids are metabolized quickly into more complex lipid species and do not accumulate.

Trafficking of Exogenous Stable Isotopically Labeled Fatty Acids into Acyl-CoA Pools in 293T-REx Cells Expressing FATP2a or FATP2b—We next assessed the trafficking of exogenous fatty acids into acyl-CoA pools using stable isotopically labeled fatty acids ([U-^{13}C]C16:0, [U-^{13}C]C18:0, [U-^{13}C]C18:1, [U-^{13}C]C18:2 (n-6), [U-^{13}C]C18:3 (n-3), [$^{2}H_{8}$]C20:4 (n-6), [$^{2}H_{5}$]C22:6 (n-3), [$^{2}H_{47}$]C24:0) in 293T-REx cells expressing FATP2a or FATP2b. These experiments were designed to address whether FATP2a, in particular, had an impact on the uptake and activation of different species of fatty acids compared with FATP2b, which is catalytically inactive. Using this approach acyl-CoAs synthesized from exogenous stable isotopically labeled fatty acids could be identified and distinguished from those generated from internal pools. We first examined the formation of acyl-CoA using 50 μM [U-^{13}C]C16:0, [U-^{13}C]C18:0, [U-^{13}C]C18:1, or [$^{2}H_{47}$]C24:0 as exogenous fatty acids. For these fatty acids, the levels of the resulting acyl-CoA were comparable between cells expressing FATP2a and FATP2b (Fig. 5, *A–C*) with the exception of the very long chain fatty acid, lignocerate, where the corresponding acyl CoA increased just over 2-fold in cells expressing FATP2a. Unique and interesting patterns started to emerge when the n-6 fatty acids [U-^{13}C]C18:2 and [$^{2}H_{8}$]C20:4 were supplied exogenously to cells expressing FATP2a or FATP2b. Arachidonyl-CoA formation in particular was increased ~30% in cells expressing FATP2a when compared with those expressing FATP2b (Fig. 6). Of significance was the finding that cells expressing FATP2a were able to form acyl-CoA derivatives from exogenous n-3 fatty acids, [U-^{13}C]C18:3 and [$^{2}H_{5}$]C22:6, to levels that were 3–5-fold higher than cells expressing FATP2b or harboring the vector alone (Fig. 7). Collectively, these data support the conclusion that FATP2a had a preference in the generation of intracellular acyl-CoAs derived from C18:3 and C22:6. More

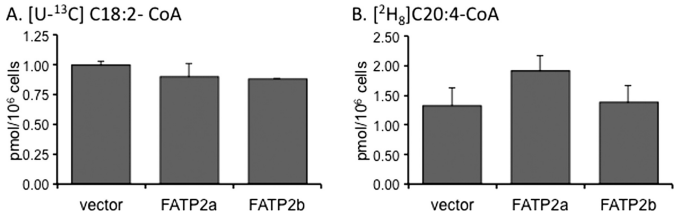

FIGURE 6. **Isotopically labeled n-6 acyl-CoA profiles in 293T-REx cells expressing FATP2a or FATP2b.** 293T-REx cells expressing FATP2a or FATP2b were labeled with 50 μM [U-^{13}C]C18:2 (*A*) or [$^{2}H_{8}$]C20:4 (*B*) for 4 h, and isotopically labeled acyl-CoAs were determined using LC-ESI/MS/MS as detailed under "Experimental Procedures." The *error bars* represent the S.E. ($n = 3$ or 4).

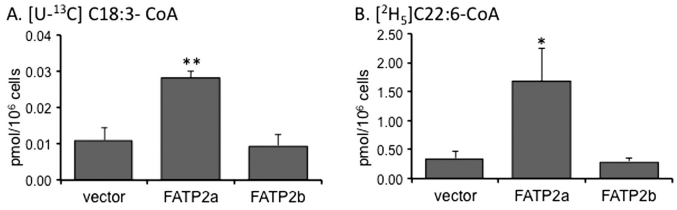

FIGURE 7. **Isotopically labeled n-3 acyl-CoA profiles in 293T-REx cells expressing FATP2a or FATP2b.** 293T-REx cells expressing FATP2a or FATP2b were labeled with 50 μM [U-^{13}C]C18:3 (*A*) or [$^{2}H_{5}$]C22:6 (*B*) for 4 h, and isotopically labeled acyl-CoAs were determined using LC-ESI/MS/MS as detailed under "Experimental Procedures." The *error bars* represent the S.E. ($n = 3$ or 4). *, $p \leq 0.05$; **, $p \leq 0.01$ relative to vector control (paired *t* test).

broadly, these findings clearly advance our understanding of members of the FATP family in general by showing particular isoforms (in this case FATP2a) provided a role in the formation of specific acyl-CoAs derived from exogenous fatty acids.

Trafficking of n-3 Acyl-CoAs into Phosphatidylcholine and Phosphatidylinositol—The finding that the expression of FATP2a increased n-3 acyl-CoAs from exogenous n-3 fatty acids provided for the first time novel insights into the specificity of an individual FATP isoform. Of interest was whether these acyl-CoAs were selectively trafficked into different classes of phospholipids. To this end, we interrogated the phosphatidylcholine and phosphatidylinositol pools after incubation of cells expressing FATP2a or FATP2b with [U-^{13}C]C18:3 or [$^{2}H_{5}$]C22:6 using ESI/MS (Figs. 8 and 9). These phospholipid classes were chosen because PC is the most abundant phospholipid in the cell and PI is known to be enriched in n-3 and n-6 fatty acids. There was no difference in [U-^{13}C]C18:3 in PC detected between cells expressing empty vector, FATP2a, or FATP2b. There was a trend for elevated [$^{2}H_{5}$]C22:6 in PC for cells expressing FATP2a but not FATP2b. In contrast, PI pools were more heavily labeled than PC pools when cells were challenged with either fatty acid species, and cells expressing FATP2a in particular caused an enrichment of both labels in PI (Fig. 9). We noted that the amount of PI labeled with [$^{2}H_{5}$]C22:6 significantly exceeded that of labeled PC by 8-fold (Table 5).

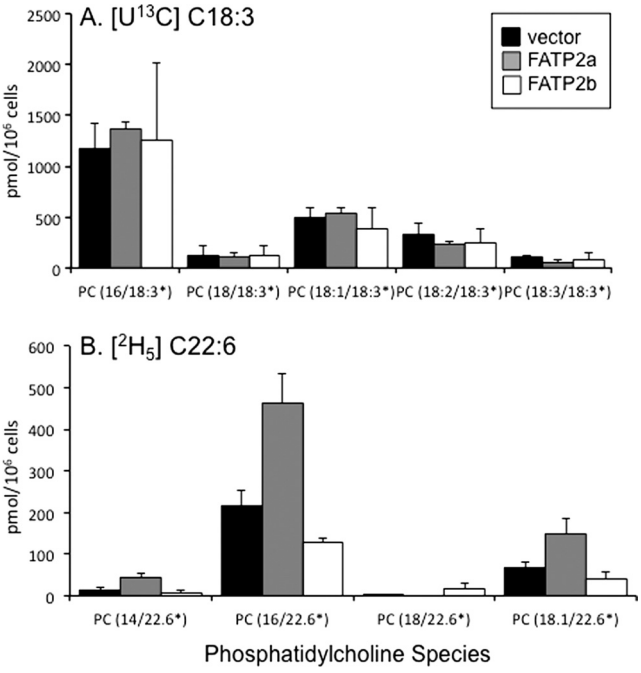

FIGURE 8. **Analysis of FATP2a (*gray bars*)- and FATP2b (*white bars*)-mediated fatty acid incorporation into phosphatidylcholine molecular species by ESI/MS.** 293T-REx cells expressing FATP2a or FATP2b were labeled with 50 μM [U-^{13}C]C18:3 (*A*) or [$^{2}H_{5}$]C22:6 (*B*) for 4 h, and isotopically labeled PC species were analyzed using ESI/MS as detailed under "Experimental Procedures." The *black bars* are control cells transformed with the vector; *error bars* represent the S.E. ($n = 3$).

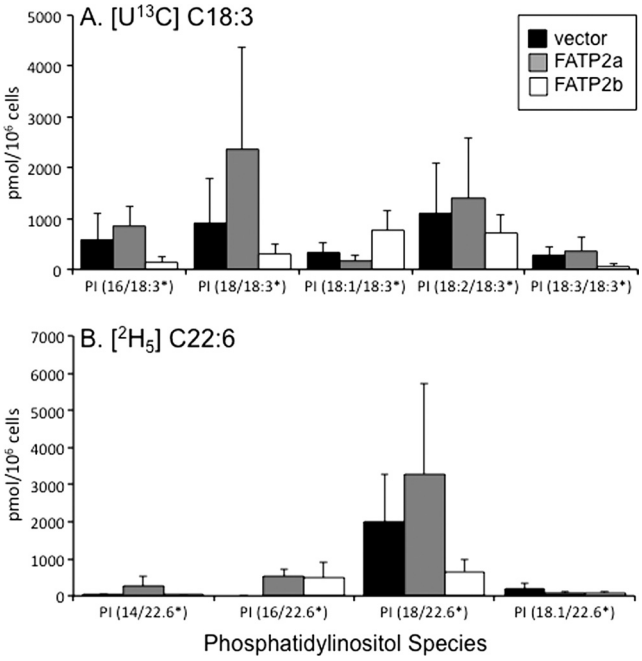

FIGURE 9. **Analysis of FATP2a (*gray bars*)- and FATP2b (*white bars*)-mediated fatty acid incorporation into phosphatidylinositol molecular species by ESI/MS.** 293T-REx cells expressing FATP2a or FATP2b were labeled with 50 μM [U-^{13}C]C18:3 (*A*) or [$^{2}H_{5}$]C22:6 (*B*) for 4 h, and isotopically labeled PI species were analyzed using ESI/MS as detailed under "Experimental Procedures." The *black bars* are control cells transformed with the vector; *error bars* represent the S.E. ($n = 3$).

DISCUSSION

In the present study we report for the first time the functional characterization of two variants of human FATP2, one of which lacks 53 amino acids from exon 3 that encodes a portion of the ATP/AMP motif required for adenylate formation. We employed two different heterologous expression systems to address the roles of these proteins in fatty acid transport and activation. Both FATP2a and FATP2b were functional in the long chain fatty acid transport pathway; FATP2a had very long chain acyl-CoA synthetase activity, whereas FATP2b was cata-

TABLE 5
Incorporation of [$^2H_5$]C22:6 and [U]^{13}C]C18:3 into phosphatidylcholine and phosphatidylinositol in 293T-REx cells expressing FATP2a

Label	PC (±S.E.)[a]	PI (±S.E.)[a]	-Fold difference (PI/PC) (±S.E.)
	%	%	
[$^2H_5$]C22:6	0.25 (0.08)	1.48 (0.40)[b]	8.19 (3.37)
[U-^{13}C]C18:3	1.02 (0.35)	1.52 (0.55)	2.21 (1.32)

[a] Numbers represent the percent of total labeled [$^2H_5$]C22:6 or [U^{13}C]C18:3 incorporated into PC and PI; $n = 3$ or 4.
[b] $p \leq 0.05$ using a paired t test relative to PC.

lytically inactive. Although these results were expected based on our previous work using alanine-scanning mutagenesis of the yeast FATP (51), the data acquired using fatty acids labeled with stable isotopes, indicating a preference for long chain polyunsaturated substrates, were not anticipated and provided novel insights into the role the fatty acid transport proteins provide in fatty acid homeostasis.

Of particular importance was the finding that FATP2a expression resulted in increased acyl-CoA formation from exogenous n-3 fatty acids and to a lesser extent the n-6 fatty acid, arachidonate. Previous work characterizing FATP2 as Acsvl1 demonstrated this enzyme had specificity for very long chain saturated fatty acids (55). This work verified these studies by showing FATP2a significantly increased intracellular lignoceryl CoA pools in response to exogenous lignocerate as a prototypical very long chain saturated fatty acid. There was no evidence from our labeling studies that FATP2a or FATP2b had a significant impact on the activation of long chain fatty acids (C16:0, C18:0, and C18:1). Thus, we propose that FATP2a functions in the fatty acid transport and activation pathways, with a preference toward the n-3 fatty acids.

The *in vivo* role of FATP2b is less clear, but the evidence provided here strongly supports a role for this protein in fatty acid uptake apart from activation as evidenced by measuring transport in both yeast and 293T-REx cells expressing FATP2b. The identification of a naturally occurring variant of FATP2, which functions in the transport of exogenous fatty acids but lacks activation activity, confirms our earlier work using alanine-scanning mutagenesis of the yeast FATP (Fat1p). Of note was the identification and characterization of the mutant form S258A-Fat1p in the ATP/AMP motif, which functioned in the transport pathway but lacked very long chain acyl-CoA synthetase activity (51). Point mutants have also been generated in the ATP/AMP motif in FATP1 and FATP4 that reduced or eliminated, respectively, fatty acid transport as measured using flow cytometry of paraformaldehyde-fixed cells after incubation with C_1-BODIPY-C_{12} (53, 57). The apparent difference in some of the results reported here and these previous publications may stem from the specific fatty acid transport assays used; in the present study we have employed a live cell real time assay to monitor the transport of the fluorescent fatty acid C_1-BODIPY-C_{12} as opposed to paraformaldehyde fixed cells and flow cytometry. Alternatively, these data may reflect specific functional differences in the different FATP isoforms.

ESI/MS analyses of stable isotopically labeled phospholipids provided novel evidence that FATP2a has a preference for activating n-3 essential fatty acids from an exogenous source, which are then trafficked preferentially into phosphatidylinositol. Interestingly, our data indicate the n-3 acyl-CoAs generated from FATP2a were channeled into non-oxidative pathways and more specifically into PI. These findings represent a significant advance in our understanding of the mechanisms that promote the selective import and trafficking of different classes of fatty acids. This work also validates the use of exogenous isotopically labeled fatty acids, which after activation are channeled into downstream metabolic pools, including complex lipids. The use of mass spectrometry to trace the formation of acyl-CoA provided important insights into the roles provided by the FATP isoforms. More specifically our finding that FATP2a preferentially promoted the formation of n-3 acyl-CoAs from exogenous fatty acids argues these proteins may function as molecular determinates in providing specificity; the resulting acyl-CoAs arising from different fatty acid species are likely to have distinct metabolic fates. Using the tools developed in the study, we are in a position to more fully address the roles provided by other members of the FATP family in fatty acid uptake, activation and trafficking, focusing on specificity in the formation of acyl-CoA and in the selective trafficking into downstream metabolic pools.

We have used RT-PCR to semiquantitatively assess the expression of both FATP2a and FATP2b in various tissues and consistently found both were expressed in placenta, liver, and intestine; we could only detect FATP2a expression in brain kidney, colon, and heart. In the tissue types where we could measure FATP2b expression, those levels were consistently low and well below the expression levels measured for FATP2a. Adipose tissue did not express either form of FATP2. Steinberg *et al.* (40), in their work describing FATP2a as Acsvl1, found that expression was most prominent in liver and kidney. Although the physiological role of FATP2 in fatty acid utilizing tissues is not well defined, there are some interesting studies that indicate this protein may function in very specialized roles in fatty acid transport and trafficking. Treatment of pregnant mice with rosiglitazone increases the expression of FATP1 and FATP4 in the placenta, which is coupled with a commensurate increase in long chain fatty acid transport (58). This treatment, however, results in marked changes in placental morphology and lowers both placenta and embryo weights when compared with mice treated with vehicle only. The most notable finding and one that was not discussed in any detail was that the expression of FATP2 was significantly reduced. When these studies are evaluated in the framework of the current study, it is worth speculating that reducing the expression of FATP2 with a peroxisome proliferator-activated receptor γ agonist results in the placental abnormalities and lowered embryo weights noted above. Perhaps in the context of placental function, the expression of FATP2 provides a mechanism for selective uptake of n-3 fatty acids that are required for fetal growth and development.

In conclusion, the current studies demonstrate for the first time that FATP2 is expressed as two alternative isoforms. Our data fur-

ther clarify the dual and distinct functions of FATP2 in long chain fatty acid uptake and very long chain fatty acid activation. The information gleaned using stable isotopically labeled fatty acids indicate a previously undisclosed role for FATP2 in the metabolism of polyunsaturated fatty acids. The approaches we have used to assess FATP2 functions may now be adapted to evaluate additional FATP isoforms to uncover unique or overlapping functions in metabolic processing of fatty acids.

Acknowledgments—We thank Drs. Hong Li, Fumin Tong, Zhenzhen Jia, and Whitney Sealls for assistance in identifying the splice variants, Dr. Elsa Arias-Barrau and Diane Singer for assistance in generating the 293T-REx stable cell lines, and Dr. Padmamalini Srinivasan for assistance in developing the mass spectrometry methods for acyl-CoA detection and quantification.

REFERENCES

1. Black, P. N., and DiRusso, C. C. (2007) *Novartis Found. Symp.* **286,** 127–138
2. Black, P. N., and DiRusso, C. C. (2007) *Biochim. Biophys. Acta* **1771,** 286–298
3. Glatz, J. F., Luiken, J. J., and Bonen, A. (2010) *Physiol. Rev.* **90,** 367–417
4. Watkins, P. A., Maiguel, D., Jia, Z., and Pevsner, J. (2007) *J. Lipid Res.* **48,** 2736–2750
5. Black, P. N., Faergeman, N. J., and DiRusso, C. C. (2000) *J. Nutr.* **130,** 305S–309S
6. DiRusso, C. C., and Black, P. N. (2004) *J. Biol. Chem.* **279,** 49563–49566
7. Overath, P., Pauli, G., and Schairer, H. U. (1969) *Eur. J. Biochem.* **7,** 559–574
8. Coleman, R. A., Lewin, T. M., Van Horn, C. G., and Gonzalez-Baró, M. R. (2002) *J. Nutr.* **132,** 2123–2126
9. Black, P. N., and DiRusso, C. C. (2003) *Microbiol. Mol. Biol. Rev.* **67,** 454–472
10. Coe, N. R., Smith, A. J., Frohnert, B. I., Watkins, P. A., and Bernlohr, D. A. (1999) *J. Biol. Chem.* **274,** 36300–36304
11. DiRusso, C. C., Connell, E. J., Faergeman, N. J., Knudsen, J., Hansen, J. K., and Black, P. N. (2000) *Eur. J. Biochem.* **267,** 4422–4433
12. DiRusso, C. C., Darwis, D., Obermeyer, T., and Black, P. N. (2008) *Biochim. Biophys. Acta* **1781,** 135–143
13. Faergeman, N. J., Black, P. N., Zhao, X. D., Knudsen, J., and DiRusso, C. C. (2001) *J. Biol. Chem.* **276,** 37051–37059
14. Faergeman, N. J., DiRusso, C. C., Elberger, A., Knudsen, J., and Black, P. N. (1997) *J. Biol. Chem.* **272,** 8531–8538
15. Gimeno, R. E., Ortegon, A. M., Patel, S., Punreddy, S., Ge, P., Sun, Y., Lodish, H. F., and Stahl, A. (2003) *J. Biol. Chem.* **278,** 16039–16044
16. Hall, A. M., Smith, A. J., and Bernlohr, D. A. (2003) *J. Biol. Chem.* **278,** 43008–43013
17. Jia, Z., Pei, Z., Maiguel, D., Toomer, C. J., and Watkins, P. A. (2007) *J. Mol. Neurosci.* **33,** 25–31
18. Marszalek, J. R., Kitidis, C., Dirusso, C. C., and Lodish, H. F. (2005) *J. Biol. Chem.* **280,** 10817–10826
19. Richards, M. R., Harp, J. D., Ory, D. S., and Schaffer, J. E. (2006) *J. Lipid Res.* **47,** 665–672
20. Schaffer, J. E. (2002) *Am. J. Physiol. Endocrinol. Metab.* **282,** E239–E246
21. Stahl, A. (2004) *Pflugers Arch.* **447,** 722–727
22. Steinberg, S. J., Mihalik, S. J., Kim, D. G., Cuebas, D. A., and Watkins, P. A. (2000) *J. Biol. Chem.* **275,** 15605–15608
23. Stremmel, W., Pohl, L., Ring, A., and Herrmann, T. (2001) *Lipids* **36,** 981–989
24. Tong, F., Black, P. N., Coleman, R. A., and DiRusso, C. C. (2006) *Arch. Biochem. Biophys.* **447,** 46–52
25. Zou, Z., Tong, F., Faergeman, N. J., Børsting, C., Black, P. N., and DiRusso, C. C. (2003) *J. Biol. Chem.* **278,** 16414–16422
26. Mashek, D. G., Li, L. O., and Coleman, R. A. (2007) *Future Lipidol.* **2,** 465–476
27. Chiu, H. C., Kovacs, A., Ford, D. A., Hsu, F. F., Garcia, R., Herrero, P., Saffitz, J. E., and Schaffer, J. E. (2001) *J. Clin. Invest.* **107,** 813–822
28. Parkes, H. A., Preston, E., Wilks, D., Ballesteros, M., Carpenter, L., Wood, L., Kraegen, E. W., Furler, S. M., and Cooney, G. J. (2006) *Am. J. Physiol. Endocrinol. Metab.* **291,** E737–E744
29. Souza, S. C., Muliro, K. V., Liscum, L., Lien, P., Yamamoto, M. T., Schaffer, J. E., Dallal, G. E., Wang, X., Kraemer, F. B., Obin, M., and Greenberg, A. S. (2002) *J. Biol. Chem.* **277,** 8267–8272
30. Igal, R. A., Wang, P., and Coleman, R. A. (1997) *Biochem. J.* **324,** 529–534
31. Bu, S. Y., and Mashek, D. G. (2010) *J. Lipid Res.* **51,** 3270–3280
32. Hatch, G. M., Smith, A. J., Xu, F. Y., Hall, A. M., and Bernlohr, D. A. (2002) *J. Lipid Res.* **43,** 1380–1389
33. Ellis, J. M., Frahm, J. L., Li, L. O., and Coleman, R. A. (2010) *Curr. Opin. Lipidol.* **21,** 212–217
34. Sun, D., Cree, M. G., and Wolfe, R. R. (2006) *Anal. Biochem.* **349,** 87–95
35. Alderson, N. L., Walla, M. D., and Hama, H. (2005) *J. Lipid Res.* **46,** 1569–1575
36. Haynes, C. A., Allegood, J. C., Sims, K., Wang, E. W., Sullards, M. C., and Merrill, A. H., Jr. (2008) *J. Lipid Res.* **49,** 1113–1125
37. Yee, J. K., Mao, C. S., Hummel, H. S., Lim, S., Sugano, S., Rehan, V. K., Xiao, G., and Lee, W. N. (2008) *J. Lipid Res.* **49,** 2124–2134
38. Kemp, S., Valianpour, F., Mooyer, P. A., Kulik, W., and Wanders, R. J. (2004) *Clin. Chem.* **50,** 1824–1826
39. Rizzo, C., Boenzi, S., Wanders, R. J., Duran, M., Caruso, U., and Dionisi-Vici, C. (2003) *Pediatr Res.* **53,** 1013–1018
40. Steinberg, S. J., Wang, S. J., Kim, D. G., Mihalik, S. J., and Watkins, P. A. (1999) *Biochem. Biophys. Res. Commun.* **257,** 615–621
41. Kaiser, C., Michaelis, S., and Mitchell, A. (1994) *Yeast Genetics*, Cold Spring Harbor Laboratory Press, Cold Spring Harbor, NY
42. Arias-Barrau, E., DiRusso, C. C., and Black, P. N. (2009) *Methods Mol. Biol.* **580,** 233–249
43. Li, H., Melton, E. M., Quackenbush, S., DiRusso, C. C., and Black, P. N. (2007) *Biochim. Biophys. Acta* **1771,** 1246–1253
44. Magnes, C., Sinner, F. M., Regittnig, W., and Pieber, T. R. (2005) *Anal Chem.* **77,** 2889–2894
45. Bligh, E. G., and Dyer, W. J. (1959) *Can J. Biochem. Physiol.* **37,** 911–917
46. Bartz, R., Seemann, J., Zehmer, J. K., Serrero, G., Chapman, K. D., Anderson, R. G., and Liu, P. (2007) *Mol. Biol. Cell* **18,** 3015–3025
47. Han, X., Abendschein, D. R., Kelley, J. G., and Gross, R. W. (2000) *Biochem. J.* **352,** 79–89
48. Liebisch, G., Drobnik, W., Reil, M., Trümbach, B., Arnecke, R., Olgemöller, B., Roscher, A., and Schmitz, G. (1999) *J. Lipid Res.* **40,** 1539–1546
49. Zhou, Z., Marepally, S. R., Nune, D. S., Pallakollu, P., Ragan, G., Roth, M. R., Wang, L., Lushington, G. H., Visvanathan, M., and Welti, R. (2011) *Lipids* **46,** 879–884
50. Hisanaga, Y., Ago, H., Nakagawa, N., Hamada, K., Ida, K., Yamamoto, M., Hori, T., Arii, Y., Sugahara, M., Kuramitsu, S., Yokoyama, S., and Miyano, M. (2004) *J. Biol. Chem.* **279,** 31717–31726
51. Zou, Z., DiRusso, C. C., Ctrnacta, V., and Black, P. N. (2002) *J. Biol. Chem.* **277,** 31062–31071
52. Stuhlsatz-Krouper, S. M., Bennett, N. E., and Schaffer, J. E. (1999) *Prostaglandins Leukot. Essent. Fatty Acids* **60,** 285–289
53. Stuhlsatz-Krouper, S. M., Bennett, N. E., and Schaffer, J. E. (1998) *J. Biol. Chem.* **273,** 28642–28650
54. Shaw, G., Morse, S., Ararat, M., and Graham, F. L. (2002) *FASEB J.* **16,** 869–871
55. Steinberg, S. J., Wang, S. J., McGuinness, M. C., and Watkins, P. A. (1999) *Mol. Genet. Metab.* **68,** 32–42
56. Deleted in proof
57. Milger, K., Herrmann, T., Becker, C., Gotthardt, D., Zickwolf, J., Ehehalt, R., Watkins, P. A., Stremmel, W., and Füllekrug, J. (2006) *J. Cell Sci.* **119,** 4678–4688
58. Schaiff, W. T., Knapp, F. F., Jr., Barak, Y., Biron-Shental, T., Nelson, D. M., and Sadovsky, Y. (2007) *Endocrinology* **148,** 3625–3634